Hyperfine structure in photoassociative spectra of $^6Li_2$ and $^7Li_2$

E. R. I. Abraham,[1] W. I. McAlexander,[1] H. T. C. Stoof,[2] and R. G. Hulet[1]
[1]*Physics Department and Rice Quantum Institute, Rice University, Houston, Texas 77251-1892*
[2]*University of Utrecht, Institute for Theoretical Physics, P.O. Box 80 006, 3508 TA Utrecht, The Netherlands*
(Received 10 October 1995)

We present spectra of hyperfine resolved vibrational levels of the $A^1\Sigma_u^+$ and $1\,^3\Sigma_g^+$ states of $^6Li_2$ and $^7Li_2$ obtained via photoassociation of colliding ultracold atoms in a magneto-optical trap. A simple first-order perturbation theory analysis accurately accounts for the frequency splittings and relative transition strengths of all observed hyperfine features. Assignment of the hyperfine structure allows accurate determination of a vibrational level center of gravity, which significantly decreases the experimental uncertainty of vibrational energies. Differences in the spectra of $^6Li_2$ and $^7Li_2$ are attributed to quantum statistics. The $1\,^3\Sigma_g^+$ series obeys Hund's case $b_{\beta S}$ coupling and the hyperfine constant is extracted for both isotopes.

PACS number(s): 33.15.Pw, 32.80.Pj, 33.20.Kf, 31.30.Gs

Photoassociative spectroscopy of ultracold atoms is a powerful technique for probing long-range, high-lying vibrational levels of diatomic molecules with high precision [1]. In this technique, a photoassociation laser is tuned to resonance between the unbound state of two colliding ground-state atoms and a bound excited-state vibrational level. For temperatures below 1 mK, which are easily attainable in laser-cooled optical traps, Doppler broadening is negligible and the spread in kinetic energies of the colliding atoms contributes an amount to the spectral width that is comparable to the natural linewidth of the transition. The high resolution inherent to this technique has enabled observations of molecular hyperfine structure in the singly excited electronic states of Li_2 [2,3], Na_2 [4–6], and Rb_2 [7,8]. Numerically calculated adiabatic potentials incorporating hyperfine interactions have aided the assignment of electronic states [9] and the modeling of line shapes [10] in the photoassociation spectrum of Na_2. In this paper, we identify the relevant hyperfine quantum numbers for photoassociative spectra of $^6Li_2$ and $^7Li_2$ reported previously [2] and show that the relative splittings and transition strengths of every hyperfine feature can be understood by simple analysis.

The initial state consists of two colliding atoms, each in the $2s$ atomic state. Let $\vec{i}_1$ represent the nuclear spin of atom 1 and $\vec{s}_1$ be its electronic spin, so that $\vec{f}_1=\vec{i}_1+\vec{s}_1$ is the total angular momentum of atom 1. Similarly, $\vec{f}_2$ is the total angular momentum of atom 2. The total molecular spin angular momentum is $\vec{G}=\vec{f}_1+\vec{f}_2$. The electronic orbital angular momentum $\vec{L}$ and the nuclear orbital angular momentum $\vec{\ell}$ combine to form the total molecular orbital angular momentum $\vec{N}$. The set of relevant quantum numbers is $|\Lambda N M_N (f_1 f_2) G M_G\rangle$, where Λ is the projection of $\vec{L}$ on the internuclear axis and M_N and M_G are the projections of $\vec{N}$ and $\vec{G}$ on a laboratory fixed axis. The initial states are superpositions of eigenstates of the total electronic spin $\vec{S}=\vec{s}_1+\vec{s}_2$, so the colliding atoms interact via both the $X\,^1\Sigma_g^+$ and the $a\,^3\Sigma_u^+$ ground-state molecular potentials. In these states, Λ is zero. At zero magnetic field, the M_N and M_G states are degenerate in energy. For simplicity, we therefore represent each initial state with just the four quantum numbers N, f_1, f_2, and G.

We consider only collisions between identical isotopes for which the eigenstates have definite symmetry upon atom exchange. Since ^7Li consists of an even number of spin-1/2 particles (seven nucleons and three electrons), it is a composite boson, while ^6Li is a composite fermion. For bosons, the eigenstates must be symmetric upon exchange, while for fermions, they must be antisymmetric. Thus only certain spin states are possible given a particular orbital state. For ^7Li, $i=3/2$, so in the $2s_{1/2}$ ground state, $f=1$ or 2, while for ^6Li, $i=1$, giving $f=1/2$ or 3/2. For both lithium isotopes, (odd) even N levels are (anti)symmetric and spin states with $G=f_1+f_2$, f_1+f_2-2, or f_1+f_2-4 are symmetric. Thus, for states where $f_1=f_2$, exchange symmetry requires $N+G$ to be even for either isotope. For states where $f_1 \neq f_2$, properly normalized and symmetrized states are $1/\sqrt{2}\,[|N f_1 f_2 G\rangle+(-1)^{N+G+1}|N f_2 f_1 G\rangle]$, which we will denote by $|N f_2 f_1 G\rangle^{\pm}$.

The atomic hyperfine interaction energies are given by $E_1=-\frac{5}{4}a_{2s}^{(7)}$ and $E_2=\frac{3}{4}a_{2s}^{(7)}$ for ^7Li and $E_{1/2}=-a_{2s}^{(6)}$ and $E_{3/2}=\frac{1}{2}a_{2s}^{(6)}$ for ^6Li, where $a_{2s}^{(7)}$ and $a_{2s}^{(6)}$ are the $2s_{1/2}$ atomic hyperfine constants for ^7Li and ^6Li, respectively. The energies are relative to the ''center of gravity'' of the $2s_{1/2}$ ground state, which would be the energy of the $2s_{1/2}$ state in the absence of hyperfine interactions. The energy of the initial free state is the sum of the energies of the colliding atoms, i.e., $E_{N f_1 f_2 G}=E_{f_1}+E_{f_2}$ if the small kinetic energy of the collision is neglected. The weak coupling between $\vec{f}_1$ and $\vec{f}_2$ is ignored, so that there is no energy dependence on G. The relevant initial energy levels for both isotopes are shown in the lower portions of Figs. 1 and 2.

The excited molecular levels observed for $^6Li_2$ and $^7Li_2$ correspond to the $A^1\Sigma_u^+$ and $1\,^3\Sigma_g^+$ singly excited states, which correlate asymptotically with the $2s_{1/2}+2p_{1/2}$ atomic states [2]. We consider vibrational levels for which the molecular interaction is large compared to the atomic spin-orbit interaction. In this Hund's case (b) regime the orbital and spin angular momenta decouple [11] and $\vec{\ell}$ again couples with $\vec{L}$ to form $\vec{N}$. The magnetic hyperfine interaction for Hund's case (b) diatomic molecules was treated theoretically by Frosch and Foley [12].

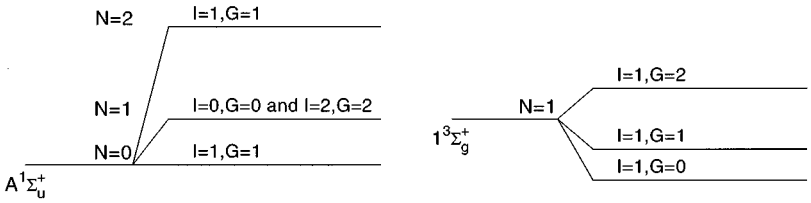

FIG. 1. Energy-level diagram for the molecular hyperfine levels of $^6Li_2$.

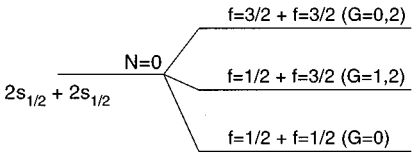

For the $1\,^3\Sigma_g^+$ excited state, the dominant hyperfine interaction is $b\vec{S}\cdot\vec{I}$, where $\vec{S}$ is the electronic spin, $\vec{I}=\vec{i}_1+\vec{i}_2$ is the nuclear spin, and b is due largely to the Fermi contact term of the $\sigma_g 2s$ orbital [13]. Since $\Lambda=0$ and the $\vec{S}\cdot\vec{N}$ and $\vec{I}\cdot\vec{N}$ interactions are small because the nuclear rotation is relatively slow, the Fermi-contact interaction dominates over all other fine and hyperfine interactions, making the total spin $\vec{G}=\vec{S}+\vec{I}$ a good quantum number ($b_{\beta S}$ coupling scheme) [12,13]. The set of relevant quantum numbers is therefore $|\Lambda N M_N(SI)GM_G\rangle$, where $\Lambda=0$ for Σ states, and M_N and M_G are again degenerate at zero magnetic field. We will represent each final state with the quantum numbers N, S, I, and G. Thus each rotational level is split into hyperfine sublevels with energies

$$E_{NSIG}=\frac{b}{2}[G(G+1)-S(S+1)-I(I+1)]. \tag{1}$$

The $b_{\beta S}$ coupling scheme has been identified in spectra of the $1\,^3\Delta_g$ state of $^7Li_2$ [14] and the $2\,^3\Sigma_g^+$, $3\,^3\Sigma_g^+$, and $4\,^3\Sigma_g^+$ states of $^7Li_2$ [15]. For the singlet states, since $S=0$, there is no first-order hyperfine splitting. The relevant ground- and excited-state energy levels are shown in Figs. 1 and 2.

Exchange symmetry requires that the eigenstates be symmetric or antisymmetric upon exchange of the identical nuclei, for nuclei of integer or half-integer spin, respectively. For $1\,^3\Sigma_g^+$ states the (odd) even N levels are (anti)symmetric and for $A\,^1\Sigma_u^+$ states the (even) odd N levels are (anti)symmetric upon exchange of nuclei [16]. The nuclear spin part of each eigenstate for $i_1=i_2$ is symmetric for $I=i_1+i_2$, i_1+i_2-2, . . . , 0.The quantity $E_{NSIG}-E_{Nf_1f_2G}$ gives the energy of a transition relative to the ground-state center of gravity, when the energy of the collision is neglected.

This analysis also gives relative transition strengths. For a dipole transition between sigma states $\Delta G=0$ and $\Delta N=\pm 1$. For a particular N to N' transition, the strength is proportional to the square of the Clebsch-Gordan coefficient between initial and final spin states

$$\frac{1}{\sqrt{2-\delta_{f_1f_2}}}[\langle f_1 f_2 G|\pm(1-\delta_{f_1f_2})\langle f_2 f_1 G|]|SIG\rangle=[(2-\delta_{f_1f_2})(2f_1+1)(2f_2+1)(2S+1)(2I+1)]^{1/2}\begin{pmatrix} s_1 & i_1 & f_1 \\ s_2 & i_2 & f_2 \\ S & I & G \end{pmatrix}, \tag{2}$$

where the large parentheses indicate a 9-j symbol. The symmetry of the 9-j symbol introduces the selection rule that $|Nf_1f_2G\rangle^+$ states will connect to excited states with $S+I+G$ odd and $|Nf_1f_2G\rangle^-$ states will connect to states with $S+I+G$ even [17]. Furthermore, the photoassociation strengths depend on the relative populations of the initial atomic hyperfine states and the $2G+1$ degeneracy for each initial quantum state with total spin G. We introduce two parameters to account for the populations of the atomic ground-state hyperfine levels: $r^{(7)}$ is the ratio of the number of atoms in the $f=2$ hyperfine level to the number of atoms in the $f=1$ hyperfine level for ^{7}Li and $r^{(6)}$ is the ratio of the number of atoms in the $f=3/2$ hyperfine level to the number of atoms in the $f=1/2$ hyperfine level for ^{6}Li.

In the experiment, lithium atoms are confined in a magneto-optical trap (MOT) [18]. The apparatus used to trap lithium is described in previous publications [2,19]. A laser beam directed through the trapped atom cloud produces photoassociation as it is tuned into resonance between an unbound state of two colliding atoms and a bound molecular

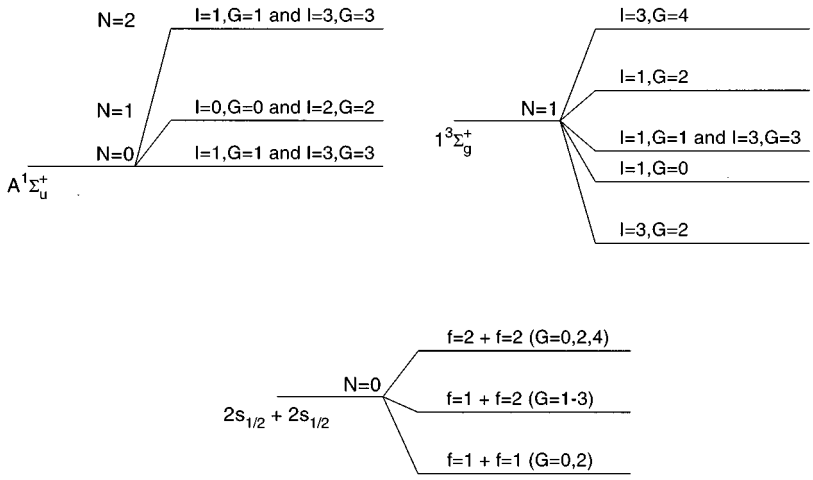

FIG. 2. Energy-level diagram for the molecular hyperfine levels of $^7Li_2$.

excited state. The excited-state molecule can radiatively decay into a bound ground-state molecule or an unbound ground state of higher kinetic energy. Both decay channels can lead to trap loss since ground-state molecules no longer interact with the trapping lasers and unbound decay products usually have sufficient energy to escape the trap. A photodiode monitors the trap-laser-induced fluorescence of the cloud of trapped atoms, which is a relative measure of the number of atoms in the trap. Photoassociation is detected as a decrease in this fluorescence.

The relative frequency of the photoassociation laser is measured using a Fabry-Pérot cavity spectrum analyzer calibrated with a Michelson-type wavemeter [2]. The MOT lifetime was between 15 and 60 s on the various days that the data were taken. Because the trap lifetime determines the rate at which the trap fills with atoms and since the detection system measures the relative number of atoms, the rate at which the photoassociation laser is scanned will affect the width and shape of the spectral features. The expected line shape of the low-frequency side of the *s*-wave photoassociation features is Boltzmann due to the thermal distribution of free atoms and zero velocity corresponds to the peak photoassociation signal [10]. The line shape of the high-frequency side of the feature should be Lorentzian as it is dominated by the natural width of the transition [10]. Since we scan the photoassociation laser from low frequency to high, this scan-time broadening has the effect of increasing the width of the high-frequency side of the feature, making the observed peaks appear more symmetrical. For the scan rates in the data presented here, 5–30 MHz per trap lifetime, this effect does not appreciably shift the peak of the signals. This was verified experimentally by changing the scan rates and is also consistent with a line-shape model that takes into account the thermal distribution, natural width, and the experimental scan-time broadening. The relative peak positions in each scan, which are the important parameters for this analysis, are unaffected by this artifact.

We have obtained 31 hyperfine and rotationally resolved spectra of 23 different vibrational levels, ranging from $v=62$ to 84, of the $1\,^3\Sigma_g^+$ state of $^7Li_2$. An example of a high-resolution spectrum with $N=1$ is shown in Fig. 3. Because of the ultralow collision energies only $N=0,1,2$ rotational levels are observed. Equation (1) was applied to the frequency splittings of each spectrum and b was allowed to vary in a least-squares fit to the data. The weighted average of the 31 independent measurements gives $b=92.4\pm0.8$ MHz. In the long-range Heitler-London approximation, where electron overlap is ignored, the hyperfine constant b can be simply related to the atomic hyperfine constants. The dominant contribution to b comes from the hyperfine interaction of the $2s_{1/2}$ ground state. In this approximation, the effective hyperfine interaction is $b_1\vec{s}_1\cdot\vec{i}_1+b_2\vec{s}_2\cdot\vec{i}_2$, where b_i is the Fermi contact interaction for each electron. Evaluated in the Heitler-London basis, where the molecular state is a superposition of equal contributions of atomic $2s$ and $2p$ states, $b_1=b_2=\frac{1}{2}a_{2s}$. The hyperfine Hamiltonian can be expressed as

$$H=\frac{a_{2s}}{2}(\vec{s}_1\cdot\vec{i}_1+\vec{s}_2\cdot\vec{i}_2)$$
$$=\frac{a_{2s}}{2}\left(\frac{1}{2}\vec{S}\cdot\vec{I}+\frac{1}{2}(\vec{s}_1-\vec{s}_2)\cdot(\vec{i}_1-\vec{i}_2)\right). \qquad (3)$$

The second term in H mixes singlet and triplet states [20] and can be neglected when the energy difference between singlet and triplet levels is large compared to the hyperfine interaction, as it is for all levels considered here. Therefore, $b\simeq\frac{1}{4}a_{2s}$ or 100.5 MHz for ^{7}Li [13]. The difference between this simple estimate and the measured value of b is presumably due to the contribution of the $2p$ orbital and to higher-order hyperfine interactions. For comparison, previous experiments on other molecular states of $^7Li_2$, where the Fermi contact term was also the dominant hyperfine interaction, found b to be 98.6 ± 4 MHz for the $1\,^3\Delta_g^+$ state [14], 96.2 ± 2 MHz for the $2\,^3\Sigma_g^+$ state, and 95.6 ± 3 MHz for the $3\,^3\Sigma_g^+$ state [15].

The simple model for transition strengths, expressed by Eq. (2), was applied to the spectrum of Fig. 3, where $r^{(7)}$ was a fitted parameter that was found to be 2.5. Previously, $r^{(7)}$ was determined for our MOT by measuring absorption of a weak probe beam for a variety of trap parameters and was found to be between 2.5 and 3.5 [21], in reasonable agreement with the best-fit value obtained here. The value of r depends on the relative optical pumping rates between the

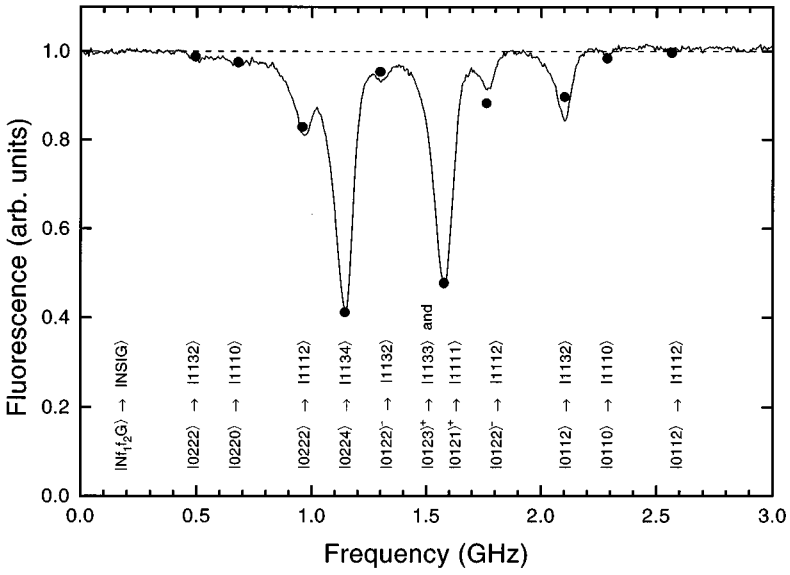

FIG. 3. Resolved hyperfine structure of the $v=64$, $N=1$ level of the $1\,^3\Sigma_g^+$ state of $^7Li_2$. Trap-laser-induced atomic fluorescence is detected as a function of photoassociation laser frequency. Transitions result in a decrease in fluorescence. The initial and final state quantum numbers for each transition are identified with the notation $|Nf_1f_2G\rangle \rightarrow |NSIG\rangle$. Due to the selection rules, $N=1$ to $N=1$ transitions are not allowed. The circles indicate the predicted relative frequency and intensity of the photoassociation signals. The dashed line indicates the base line for the calculated signal intensities. The transitions $|0123\rangle^+ \rightarrow |1133\rangle$ and $|0121\rangle^+ \rightarrow |1111\rangle$ are degenerate and the corresponding transition strength is calculated to be the sum of the strengths of the respective transitions. For this spectrum, $b=91.5\pm2.2$ MHz and $r^{(7)}=2.5$.

ground-state levels produced by the trapping lasers and is not necessarily equal to the statistical ratio 5/3. Because of the effect of quantum statistics, only excited states with $I=1$ or 3 are observed.

Hyperfine structure is also resolved for the $1\,^3\Sigma_g^+$ state of $^6Li_2$ where 16 spectra of 9 different vibrational levels ($v=59$–73) were obtained. To our knowledge, these are the first hyperfine resolved spectra of $^6Li_2$. An example is shown in Fig. 4. Again, a least-squares fit of b is done to reproduce the frequency splittings and $r^{(6)}$ is fit to reproduce the relative transition strengths. The weighted average of b for the 16 independent spectra is 39.4 ± 0.9 MHz, which can be compared with $\frac{1}{4}a_{2s}^{(6)}=38.0$ MHz. The value of $r^{(6)}$ is found to be 2.0 for the spectrum in Fig. 4, which compares well with a previous absorption measurement for similar trap conditions which resulted in $r^{(6)}\simeq2$. Again, the effect of quantum statistics is evident in the spectra, as only transitions to excited states with $I=1$ are observed.

There is no excited-state hyperfine structure for the $A\,^1\Sigma_u^+$ state. A high-resolution scan of one vibrational level for $^7Li_2$ is shown in Fig. 5. Rotational structure and structure due to the ground-state hyperfine splittings are evident. It has been predicted that the effect of a d-wave resonance may be observed in the photoassociative spectra of the $A\,^1\Sigma_u^+$ state

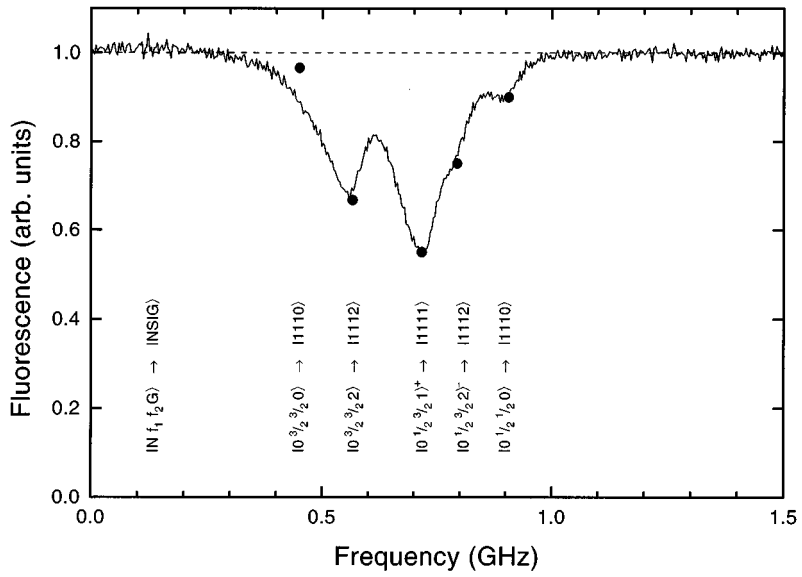

FIG. 4. Resolved hyperfine structure of the $v=64$, $N=1$ level of the $1\,^3\Sigma_g^+$ state of $^6Li_2$; the the notation is the same as in Fig. 3. For this spectrum, $b=39\pm3$ MHz and $r^{(6)}=2.0$.

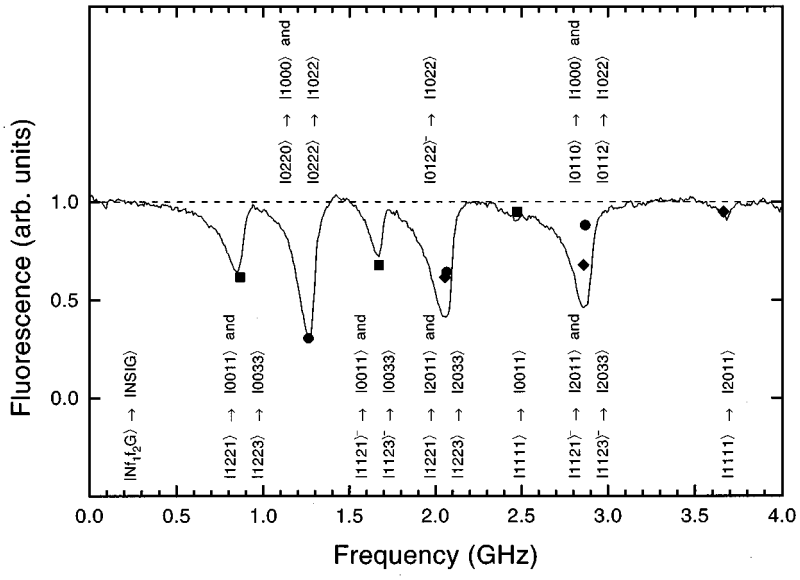

FIG. 5. Hyperfine and rotational structure of the $v=89$ level of the $A\ ^1\Sigma_u^+$ state of $^7Li_2$. The predicted relative frequency and intensity of the photoassociation signals are shown with squares for transitions involving $N=0$ final states, circles for $N=1$ final states, and diamonds for $N=2$. The $N=0$ to $N=1$, $N=1$ to $N=0$, and $N=1$ to $N=2$ transitions are normalized separately. Degenerate transitions are summed as described in Fig. 3. The rotational splittings are given by $BN(N+1)$, where B is the rotational constant that is fit to the data. The rotational splitting between the $N=1$ and $N=2$ levels for this vibrational level is coincidentally nearly the same as the ground-state atomic hyperfine splitting. For this spectrum, $r^{(7)}=2.6$ and $B=0.198$ GHz.

of $^7Li_2$, for collision energies near 16 mK [22,23]. While we observe no evidence of the resonance in this spectra, it is reasonable to assume that the atomic gas is too cold, since a previous time-of-flight measurement gave a temperature of 2 mK [24]. A high-resolution scan of one vibrational level for the $A\ ^1\Sigma_u^+$ state of $^6Li_2$ is shown in Fig. 6. Rotational structure and structure due to the ground-state level splittings are evident. With hyperfine splittings smaller than that for $^7Li_2$, the rotational structure is completely resolved.

We have identified all rotational and hyperfine features observed in high-resolution photoassociative spectra of the $1\ ^3\Sigma_g^+$ and $A\ ^1\Sigma_u^+$ states of $^6Li_2$ and $^7Li_2$ using a simple first-order perturbation theory analysis for both the relative splittings and intensities of the hyperfine levels. First-order perturbation theory is appropriate for this system because the molecular levels under investigation exist primarily in the long-range asymptotic regime, where electron wave-function overlap is small. Furthermore, there are no nearby degenerate levels of different molecular states that could perturb the observed levels. The usefulness of the first-order perturbation theory for analyzing hyperfine structure of long-range molecular states was also recently demonstrated for the highest vibrational levels of the Na_2 ground state in comparisons with a coupled-channels calculation in the hyperfine basis

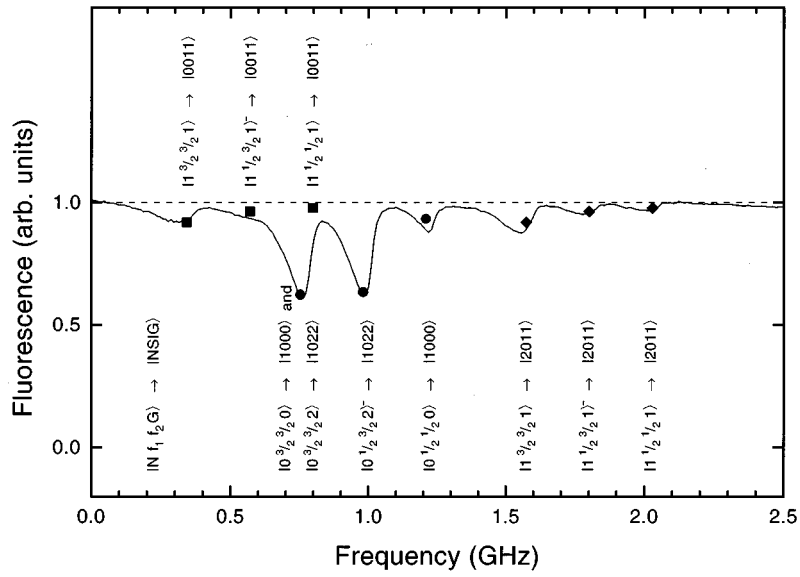

FIG. 6. Hyperfine and rotational structure of the $v=83$ level of the $A\ ^1\Sigma_u^+$ state of $^6Li_2$. As in Fig. 5, squares denote transitions involving $N=0$ final states, circles for $N=1$, and diamonds for $N=2$. For this spectrum, $r^{(6)}=2.2$ and $B=0.205$ GHz.

[20]. This ability to identify hyperfine structure will facilitate more accurate determinations of the energies of vibrational levels, which when combined with recent spectroscopic data on the lower vibrational levels of the $A\ ^1\Sigma_u^+$ state of $^6Li_2$ [25] will allow for more accurate extraction of atomic dipole moments from photoassociative spectra [26].

We gratefully acknowledge helpful discussions with R. Field, P. Julienne, and C. Williams. This work has been supported by the National Science Foundation and the Robert A. Welch Foundation. W.I.M. received support from the Fannie and John Hertz Foundation.

[1] P. D. Lett, P. S. Julienne, and W. D. Phillips, Annu. Rev. Phys. Chem. **46**, 423 (1995), and references therein.
[2] E. R. I. Abraham, N. W. M. Ritchie, W. I. McAlexander, and R. G. Hulet, J. Chem. Phys. **103**, 7773 (1995).
[3] W. I. McAlexander, E. R. I. Abraham, N. W. M. Ritchie, C. J. Williams, H. T. C. Stoof, and R. G. Hulet, Phys. Rev. A **51**, R871 (1995).
[4] P. D. Lett, K. Helmerson, W. D. Phillips, L. P. Ratliff, S. L. Rolston, and M. E. Wagshul, Phys. Rev. Lett. **71**, 2200 (1993).
[5] L. P. Ratliff, M. E. Wagshul, P. D. Lett, S. L. Rolston, and W. D. Phillips, J. Chem. Phys. **101**, 2638 (1994).
[6] V. S. Bagnato, J. Weiner, P. S. Julienne, and C. J. Williams, Laser Phys. **4**, 1062 (1994).
[7] J. D. Miller, R. A. Cline, and D. J. Heinzen, Phys. Rev. Lett. **71**, 2204 (1993).
[8] R. A. Cline, J. D. Miller, and D. J. Heinzen, Phys. Rev. Lett. **73**, 632 (1994).
[9] C. J. Williams and P. S. Julienne, J. Chem. Phys. **101**, 2634 (1994).
[10] R. Napolitano, J. Weiner, C. J. Williams, and P. S. Julienne, Phys. Rev. Lett. **73**, 1352 (1994).
[11] G. Herzberg, *Spectra of Diatomic Molecules*, 2nd ed. (Van Nostrand Reinhold, New York, 1950).
[12] R. A. Frosch and H. M. Foley, Phys. Rev. **88**, 1337 (1952).
[13] L. Li, Q. Zhu, and R. W. Field, J. Mol. Spectrosc. **134**, 50 (1989).
[14] L. Li, T. An, T.-J. Wang, A. M. Lyyra, W. C. Stwalley, R. W. Field, and R. A. Bernheim, J. Chem. Phys. **96**, 3342 (1992).
[15] A. Yiannopoulou, K. Urbanski, A. M. Lyyra, L. Li, B. Ji, J. T. Bahns, and W. C. Stwalley, J. Chem. Phys. **102**, 3024 (1995).
[16] I. N. Levine, *Molecular Spectroscopy* (Wiley, New York, 1975), p. 182.
[17] R. N. Zare, *Angular Momentum* (Wiley, New York, 1988).
[18] E. L. Raab, M. Prentiss, A. Cable, S. Chu, and D. E. Pritchard, Phys. Rev. Lett. **59**, 2631 (1987).
[19] N. W. M. Ritchie, E. R. I. Abraham, Y. Y. Xiao, C. C. Bradley, R. G. Hulet, and P. S. Julienne, Phys. Rev. A **51**, R890 (1995).
[20] A. J. Moerdijk and B. J. Verhaar, Phys. Rev. A **51**, R4333 (1995).
[21] N. W. M. Ritchie, Ph.D. thesis, Rice University, 1994 (unpublished).
[22] J. N. R. Côté, Ph.D. thesis, Massachusetts Institute of Technology, 1994 (unpublished).
[23] The effect of a *d*-wave resonance in photoassociation of ^{87}Rb was recently observed by H. M. J. M. Boesten, C. C. Tsai, J. R. Gardner, D. J. Heinzen, and B. J. Verhaar (unpublished).
[24] Y. Y. Xiao, Master's thesis, Rice University, 1993 (unpublished).
[25] C. Linton, F. Martin, A. J. Ross, I. Russier, P. Crozet, S. Churassy, and R. Bacis, J. Mol. Spectrosc. (to be published)
[26] W. I. McAlexander, E. R. I. Abraham, and R. G. Hulet (unpublished).